

Deregulated Cdk5 promotes oxidative stress and mitochondrial dysfunction

Kai-Hui Sun,* Yolanda de Pablo,* Fabien Vincent*[†] and Kavita Shah*

*Department of Chemistry and Purdue Cancer Center, Purdue University, West Lafayette, IN 47907, USA

[†]Renovis, Inc., South San Francisco, California, USA

Abstract

Oxidative stress is one of the earliest events in Alzheimer's disease (AD). A chemical genetic screen revealed that deregulated cyclin-dependent kinase 5 (Cdk5) may cause oxidative stress by compromising the cellular anti-oxidant defense system. Using novel Cdk5 modulators, we show the mechanism by which Cdk5 can induce oxidative stress in the disease's early stage and cell death in the late stage. Cdk5 dysregulation upon neurotoxic insults results in reactive oxygen species (ROS) accumulation in neuronal cells because of the inactivation of peroxiredoxin I and II. Sole temporal activation of Cdk5 also increases ROS, suggesting its major role in this process. Cdk5 inhibition rescues mitochondrial damage upon neurotoxic insults, thereby revealing Cdk5 as an *upstream* regulator of mitochondrial dysfunction.

Alzheimer's disease (AD) is a fatal neurodegenerative disorder that is characterized by two major hallmarks: β -amyloid (A β) plaques and neurofibrillary tangles (NFTs) with profound death in specific areas of the brain. However, it is unclear whether A β plaques and NFTs represent a cause, an effect or the end phase in the disease's pathology. The molecular mechanism leading to extensive cell death remains to be fully elucidated.

Extensive recent literature supports oxidative stress, mitochondrial dysfunction, and calcium dyshomeostasis as the early contributors in AD pathology that occur prior to the development of detectable plaques and tangles (Nunomura *et al.* 1999, 2000, 2001; Pratico *et al.* 2001; Lee *et al.* 2005). Notably, both A β and glutamate induce neurotoxicity via enhanced oxidative stress (Lafon-Cazal *et al.* 1993; Schulz *et al.* 2000), mitochondrial dysfunction (Castilho *et al.* 1999), and calcium dyshomeostasis (Schinder *et al.* 1996).

Both A β - and glutamate-induced toxicities in neurons are largely dependent on cyclin-dependent kinase (Cdk5) (Alvarez *et al.* 1999; Lee *et al.* 2000; Wei *et al.* 2002; O'Hare *et al.* 2005). Cdk5, a serine-threonine kinase, belongs to the

As mitochondrial damage results in elevated ROS and Ca²⁺ levels, both of which activate Cdk5, we propose that a feedback loop occurs in late stage of AD and leads to cell death (active Cdk5 \rightarrow ROS \rightarrow excess ROS \rightarrow mitochondrial damage \rightarrow ROS \rightarrow hyperactive Cdk5 \rightarrow severe oxidative stress and cell injury \rightarrow cell death). Cdk5 inhibition upon neurotoxic insult prevents cell death significantly, supporting this hypothesis. As oxidative stress and mitochondrial dysfunction play pivotal roles in promoting neurodegeneration, Cdk5 could be a viable therapeutic target for AD.

Keywords: Alzheimer's disease, cyclin-dependent kinase 5, oxidative stress, peroxiredoxin I, peroxiredoxin II, reactive oxygen species.

J. Neurochem. (2008) **107**, 265–278.

Cdk family (Beaudette *et al.* 1993). Unlike other Cdks which are activated by binding to cyclin partners, Cdk5 is activated by neuron-specific, membrane-localized co-activators, p35 and p39. Cdk5 is hyperactivated upon oxidative stress, mitochondrial dysfunction, excitotoxicity, A β exposure, calcium dyshomeostasis and inflammation, all of which are critical in AD (Tsai *et al.* 1994; Patrick *et al.* 1999; Lee *et al.*

Received June 5, 2008; revised manuscript received July 31, 2008; accepted August 1, 2008.

Address correspondence and reprint requests to Kavita Shah, Department of Chemistry, Purdue University, 560 Oval Drive, West Lafayette, IN 47907, USA. E-mail: shah23@purdue.edu

Abbreviations used: AD, Alzheimer's disease; A β , β -amyloid; Cdk, cyclin-dependent kinase; CIP, Cdk5 inhibitory peptide; DCFDA, 2',7'-dichlorofluorescein diacetate; DIV, days *in vitro*; DMEM, Dulbecco's modified Eagle's medium; DMSO, dimethylsulfoxide; FBS, fetal bovine serum; JC-1, 5,5',6,6'-tetrachloro-1,1',3,3'-tetraethylbenzimidazolylcarbocyanine iodide; mPlum-RFP, m-Plum-Red fluorescent protein; MTT, 3-(4,5-dimethylthiazol-2-yl)-2,5-diphenyltetrazolium bromide; NFT, neurofibrillary tangles; NGF, nerve growth factor; PBS, phosphate-buffered saline; Prx, peroxiredoxin; ROS, reactive oxygen species; SDS, sodium dodecyl sulfate.

2000; Dhavan and Tsai 2001; Stocchi *et al.* 2003; Cruz and Tsai 2004; Quintanilla *et al.* 2004; Shea *et al.* 2004; Kitazawa *et al.* 2005). These neurotoxic stimuli activate calpain which cleaves Cdk5 activator p35 (or p39) into p25 (or p29). These pathological activators not only transform Cdk5 into a 'hyperactive' kinase, but also change its subcellular localization from particulate to cytosolic and nuclear, which triggers various events associated with neurodegeneration (Lau and Ahljianian 2003; Monaco 2004; Smith *et al.* 2004). Although, significant higher activity of Cdk5 has been observed in AD brains compared with non-demented control brains, the relative levels of p25 in AD versus healthy brains remains a contentious issue (Lee *et al.* 1999; Patrick *et al.* 1999; Taniguchi *et al.* 2001; Yoo and Lubec 2001; Tseng *et al.* 2002; Tandon *et al.* 2003; Swatton *et al.* 2004).

Initially, we investigated Cdk5's role in AD using a chemical genetic screen which enables unbiased identification of a kinase's direct substrates in a global environment. Peroxiredoxin-I (Prx-I) and peroxiredoxin-II (Prx-II) were identified as direct substrates of Cdk5 from mouse brain lysates. Prx-I and Prx-II belong to the Prx family of peroxidases that efficiently scavenge cellular reactive oxygen species (ROS) (Mizusawa *et al.* 2000; Chang *et al.* 2002; Kang *et al.* 2005; Veal *et al.* 2007). Identification of Prx-I and Prx-II as Cdk5 substrates suggested that Cdk5 deregulation may maintain sustained oxidative stress in AD by compromising the cellular anti-oxidant defense system. A recent study identified Prx-II as a substrate of Cdk5 and showed the kinase's involvement in Parkinson's disease *downstream* of mitochondrial dysfunction upon MPTP stimulation (Qu *et al.* 2007). However, Cdk5's role in promoting oxidative stress in AD has not been elucidated.

Oxidative stress and dysfunctional mitochondria are among the earliest events in AD (Nunomura *et al.* 2001). Oxidative stress causes DNA damage, protein and lipid peroxidation, protein aggregation, mitochondrial dysfunction, microglial and astrocyte activation, inflammation, proteasome malfunction, and cell death (Zhu *et al.* 2007). Damaged mitochondria also trigger abnormal onset of neuronal degeneration and cell death in AD (Moreira *et al.* 2007). If cell death cascades are blocked downstream of mitochondria, death can only be delayed. To evaluate Cdk5 as a target for neuroprotective strategies, knowing whether Cdk5 deregulation *precedes* mitochondrial dysfunction is crucial. Thus, the three key questions which this study aims to tackle are: (i) can Cdk5 deregulation alone or downstream of A β and glutamate cause oxidative stress, and is it because of Prx-I and Prx-II?; (ii) Is Cdk5 an upstream regulator or a downstream effector of mitochondrial depolarization?; (iii) whether Cdk5 inhibition alleviates or delays cell death following neurotoxic insults.

Novel genetic tools TAT-fused p25 (TAT-p25, activator) and TAT-fused Cdk5 inhibitory peptide (TAT-CIP) developed

in our laboratory (Sun *et al.* 2008) were used to specifically activate or inhibit Cdk5 activity with high temporal control. TAT is an 11-mer peptide sequence from residues 47–57 of HIV-Tat (YGRKKRRQRRR). CIP is a 126-residue artificial peptide containing p35^{154–279}, which inhibits Cdk5 specifically and potently by blocking Cdk5/p25 complex formation when expressed endogenously (Amin *et al.* 2002; Zheng *et al.* 2002, 2005). TAT peptide derived from human immunodeficiency virus TAT sequence allows fast and efficient transduction of the recombinant proteins into the cells (Nagahara *et al.* 1998; Becker-Hapak *et al.* 2001). With the aid of these tools, we show that Cdk5 directly causes excessive oxidative stress and mitochondrial dysfunction in neurons leading to cell death, downstream of A β and glutamate, both of which play key roles in AD pathology.

Experimental procedures

Materials

Glutamate, 3-(4,5-dimethyl-diazol-2-yl)-2,5-diphenyltetrazolium bromide (MTT) and poly-L-lysine were obtained from Sigma (St Louis, MO, USA). A β ^{25–35}, 5,5',6,6'-tetrachloro-1,1',3,3'-tetraethylbenzimidazolylcarbocyanine iodide (JC-1), and 2',7'-dichlorofluorescein diacetate (DCFDA) were purchased from Anaspec (San Jose, CA, USA). Roscovitine was purchased from LC laboratory (Woburn, MA, USA). Antibody for p35/p25 (C-19), actin (C-2), and Prx (L-20) was purchased from Santa Cruz Biotechnology (Santa Cruz, CA, USA). Nerve growth factor (NGF) was obtained from Austral Biologicals (San Ramon, CA, USA).

Cloning, expression and purification of Cdk5, Cdk5 (F80G), and p25

The mutant Cdk5 protein (F80G) (Cdk5-as1) construct was generated from Cdk5 in pGEX-2T bacterial expression system using the Quickchange™ protocol from Qiagen (Valencia, CA, USA) according to the manufacturer's instructions. Cdk5-as1 and p25 cDNA were transformed in BL21-Gold cells (Stratagene, La Jolla, CA, USA), expressed, and purified using glutathione agarose beads as reported before (Shah *et al.* 1997).

Kinase assays using [γ -³²P] N⁶-phenethyl ATP

N⁶-phenethyl ATP was synthesized as described before (Shah and Shokat 2002). For *in vitro* labeling of proteins, 10 μ g of lysate was added into kinase buffer (20 mM HEPES, pH 7.5, 50 mM NaCl, and 10 mM MgCl₂). One micromolar of ATP was then added to the reaction and incubation was carried out for 10 min at 25°C. The kinase complex was subsequently added and the kinase reactions were initiated immediately by adding 0.5 μ Ci of [γ -³²P] ATP or [γ -³²P] N⁶-phenethyl ATP. Reactions were terminated by adding sodium dodecyl sulfate (SDS) sample buffer and boiled for 5 min, labeled proteins were separated on 8–12% gradient SDS-polyacrylamide gel electrophoresis gel and were transferred to Immobilon-P nylon membrane (Millipore Corporation, Bedford, MA, USA) by electroblotting. For autoradiography, the membrane was exposed to the Phospho screen overnight and visualized by Storm860 (Molecular Dynamics, Sunnyvale, CA, USA).

³²P orthophosphoric acid labeling

Either vector or p25 was co-transfected with either myc-tagged-Prx-I or myc-tagged-Prx-II in HeLa cells using lipofectamine (Invitrogen, Carlsbad, CA, USA). After 24 or 36 h, cells were washed with phosphate-free Dulbecco's modified Eagle's medium (DMEM), supplemented with 5% dialyzed fetal bovine serum (FBS) (Hyclone, Logan, UT, USA), followed by incubation in the same media for 1 h. Eleven microliter of ³²P-orthophosphoric acid (150 mCi/mM, Perkin Elmer) was next added and the cells were further incubated for 4 h at 37°C. Supernatant was removed and the cells were washed twice with phosphate-buffered saline (PBS). The cells were lysed in 0.75 mL of lysis buffer A [(1% NP-40, 0.15 M NaCl, 10 mM Na₃PO₄, pH 7.5, 2 mM EDTA, 50 mM NaF, 0.1% deoxycholate, 0.1% SDS, protease inhibitors, and phosphatase inhibitor cocktail 1 and 2 (Sigma)] and the resulting lysate was centrifuged for 10 min at 25°C. Prx I and Prx II immune complexes were isolated using 9E10 myc antibody (Santa Cruz Biotechnology) and protein G sepharose beads for 4 h at 4°C. The proteins were separated on 16% SDS-polyacrylamide gel electrophoresis gel, electrophoretically transferred to polyvinylidene fluoride membrane, and were exposed to Kodak Biomax MS film (Sigma) with a Biomax MS intensifying screen at -70°C.

Expression plasmids and constructs

pET-28b-TAT (V2.1) and pTAT-HA vectors were gifts from Steve Dowdy. m-Plum-Red fluorescent protein (mPlum-RFP) was a gift from Roger Tsien. p25, CIP, and mPlum-RFP were cloned into pET-28b-TAT (V2.1) vector to generate TAT-fusion proteins. TAT-fusion-Prx-I (TAT-Prx-I), Prx-I (T90A) mutant [TAT-Prx-I (T90A)], Prx-II (TAT-Prx-II), and Prx-II (T89A) mutant [TAT-Prx-II (T89A)] were created using overlapping PCR in pTAT-HA vector.

Expression and purification of TAT-fusion proteins

TAT-fusion proteins were expressed and purified as described previously (Sun *et al.* 2008). Protein concentration was determined by a Bradford assay and the protein purity was assessed by gel electrophoresis. All expressed TAT-fusion proteins were verified by western blotting using 6-His antibodies. Imidazole was used to elute TAT-fusion proteins from Ni-NTA beads, so same amount of elution buffer was added in the control treatments.

Cdk5 kinase assay

Glutamate or TAT-fusion protein-treated cells were rinsed twice with cold PBS and lysed in 1% NP-40 lysis buffer (1% NP-40, 20 mM Tris, pH 8.0, 150 mM NaCl, 1 mM phenylmethylsulfonyl fluoride, 10 µg/mL leupeptin, and 10 µg/mL aprotinin). Cleared lysates were mixed with Cdk5 antibody and protein A sepharose beads (Sigma) and incubated at 4°C for 2 h followed by *in vitro* Cdk5 kinase assay as previously described (Sun *et al.* 2008).

In vitro phosphorylation of Prx by Cdk5/p25 complex and peroxidase assay

Recombinant Prx-I and Prx-II (5 µg each) were phosphorylated by the purified Cdk5/p25 complex (20 ng) at 30°C in a final volume of 30 µL containing 50 mM Tris, pH 8.0, 20 mM MgCl₂, 100 µM ATP, respectively, followed by peroxidase assay as described previously (Thunman *et al.* 1972; Jiang *et al.* 2005).

Cell culture

HT22 cells were a gift from David Schubert (Salk Institute, San Diego, CA, USA). HT22 cells were cultured in DMEM supplemented with 10% FBS. PC12 cells were grown in DMEM with 10% FBS and 5% horse serum.

Isolation of primary cortical cells

Time pregnant CD-1 mice were purchased from Charles River (Wilmington, MA, USA). Primary cortical neurons were isolated from E17 CD-1 mouse embryos as described previously (Behrens *et al.* 1999; Sun *et al.* 2008). After 3 days *in vitro* (DIV), 10 µM cytosine arabinoside was added to prevent glial proliferation. Under these conditions less than 5% of total cells were astrocytes. Cultures were maintained at 37°C in a humidified 5% CO₂ atmosphere. All experiments were conducted on 5 and 6 DIV.

DCFDA staining and cytometry

For ROS measurement in HT22 cells, 10⁵ cells were plated per well in a six-well plate for 12 h. For primary neurons, 3 × 10⁵ cortical cells were plated for at least 4 days. Roscovitine (10 µM), TAT-CIP (200 nM), TAT-RFP (200 nM), or the vehicle [0.1% dimethylsulfoxide (DMSO) or 0.1 mM imidazole] were added 30 min prior to the neurotoxic stimuli. After the treatment, ROS production was measured by DCFDA staining using a FACScalibur as described previously (Sun *et al.* 2008).

Mitochondria polarization measurement

PC12 cells were plated at 10⁵ cells per well, serum-starved overnight and differentiated for 5 days with 50 ng/mL NGF in the presence of 0.5% FBS. After various treatments as described in the figure legend, 0.8 µg/µL of JC-1 was added from a 40 µg/µL stock solution in DMSO. Cells were incubated at 37°C for 10 min and then gently detached by pipetting. Cell suspensions were spun and resuspended in PBS supplemented with 0.5% bovine serum albumin right before the measurement using a FACScalibur. For imaging, HT22 cells were plated on poly-L-Lys pre-coated Labtek eight-well chambered coverglass at a 10 000 cells/cm² confluence. After 12 h cells were treated for 20 min with 200 nM TAT-CIP or 0.5 mM imidazole and then 10 mM glutamate for 10 h. Recombinant protein or imidazole buffer were re-added every 4 h. At the end of the treatment, media was changed to PBS with 0.8 µg/µL JC-1 and incubated for 10 min at 37°C. JC-1 was removed and PBS was added for the confocal imaging. Pictures from red and green fluorescence were taken in a Nikon TE2000 inverted confocal microscope (Nikon, Tokyo, Japan) with a Radiance 2100MP Rainbow Laser (Bio-Rad Laboratories). Representative images were taken from each sample. Percentage of cells with depolarized mitochondria was counted as the average of 100 cells from at least five random fields.

MTT assay

HT22 cells were seeded onto 12-well plates at 25 000 cells per well overnight, pre-treated for 30 min either with DMSO (vehicle of roscovitine) or roscovitine (10 µM) or sustained addition of imidazole (vehicle of TAT-fusion proteins) or TAT-CIP (200 nM) (every 4 h) followed by the 10 mM glutamate treatment. After 18 h, MTT assay was conducted as described previously (Sun *et al.* 2008).

Nuclear staining using propidium iodide

HT22 cells plated on coverslips were treated with 10 mM glutamate along with either 10 μ M roscovitine, 0.02% DMSO, sustained addition of 200 nM TAT-CIP or 0.1 mM imidazole (every 4 h) for 12 h. After the treatment, nuclear staining using propidium iodide was conducted as described previously (Sun *et al.* 2008).

Statistical analysis

Bar graph results were plotted as the average \pm SEM. Probability values were calculated from one-way ANOVA followed by *post hoc* analysis and displayed as: * $p < 0.05$, ** $p < 0.01$, *** $p < 0.001$ when comparing data to the control. # was used when comparing data to glutamate or A β treatment.

Results

Chemical genetic screen

Identification of direct substrates of Cdk5 in mouse brain using a chemical genetic approach

Identification of Cdk5's direct substrates in the brain is important to understand its function at the highest resolution. A chemical genetic approach which can identify direct substrates of protein kinases was utilized in this study (Shah *et al.* 1997; Shah and Shokat 2002, 2003; Shah and Vincent 2005; Kim and Shah 2007; Sun *et al.* 2008). The kinase of interest is engineered to accept a non-natural phosphate donor substrate (ATP*) that is poorly accepted by wild-type protein kinases in the cell. A unique active site pocket in the ATP binding site of the target kinase is created by the replacement of a conserved bulky residue with glycine or alanine. A complementary substituent on ATP is created by

attaching bulky substituents at the *N*-6 position of ATP (e.g., *N*⁶-benzyl ATP, *N*⁶-phenethyl ATP, etc.). As the ATP analog is not accepted by other wild-type kinases in the cells, this strategy allows unbiased identification of direct substrates of any kinase in a global environment. This chemical genetic approach was used in conjunction with 2D electrophoresis and mass spectrometry to identify the direct substrates of Cdk5 in mouse brain extracts.

An analog-sensitive mutation was created in the active site of Cdk5 by replacing F80 with a glycine residue (Cdk5-analog sensitive kinase-1, Cdk5-as1). To identify the most optimal orthogonal phospho-donor for the engineered kinase, several [γ -³²P] ATP analogs were synthesized and screened using wt Cdk5/p25 and Cdk5-as1/p25 kinases. Our results established [γ -³²P] *N*⁶-phenethyl ATP as the optimal orthogonal phosphodonor for Cdk5-as1 kinase.

Identification of direct substrates of Cdk5 in mouse brain

Cdk5-as1 phosphorylates its direct substrates in the presence of other kinases using [γ -³²P] phenethyl ATP (compare lanes 2 and 3 in Fig. 1a). To identify the direct substrates of Cdk5 in mouse brain lysate, an *in vitro* kinase reaction was performed in the presence of orthogonal [γ -³²P] *N*⁶-phenethyl ATP and the proteins were separated using 2D gel. Although more than 50 proteins were phosphorylated in a Cdk5-dependent manner, hardly any showed a distinct coomassie staining, suggesting that most Cdk5 substrates were less abundant. We were unable to identify any of these proteins by mass spectral analysis.

To overcome this problem, mouse brain lysate was fractionated using both anion and cation exchange columns.

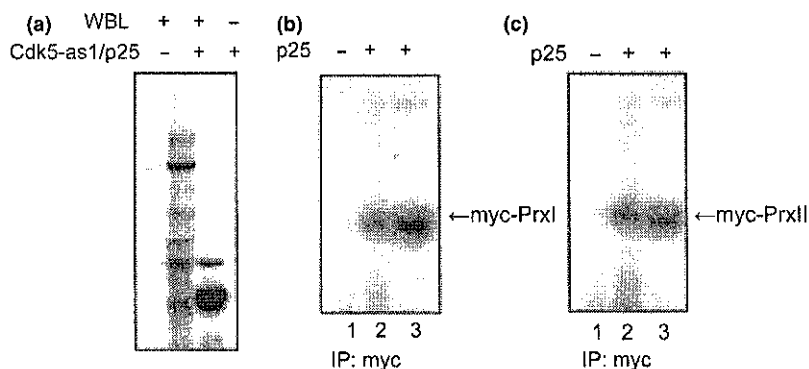


Fig. 1 Prx-I and Prx-II are direct substrates of Cdk5. (a) Cdk5-as1 specifically uses [γ -³²P]-*N*⁶-phenethyl ATP and phosphorylates its direct substrates in whole mouse brain lysates (WBL). Autoradiogram of labeled proteins after incubation of WBL (lanes 1 and 2) with [γ -³²P]-*N*⁶-phenethyl ATP in the absence (lane 1) or presence of Cdk5-as1 and p25 (lane 2). Lane 3 shows phosphorylation of Cdk5 and p25. (b) *In vivo* [γ -³²P] orthophosphoric acid labeling experiment shows Prx-I as a cellular substrate of Cdk5/p25. p25 and Myc-tagged Prx-I were co-transfected in HeLa cells and expressed for either 24

or 36 h (lanes 2 and 3 respectively) followed by ³²P-orthophosphoric acid radiolabeling and immunoprecipitated as described in Experimental procedures. (c) *In vivo* [γ -³²P] orthophosphoric acid labeling experiment shows Prx-II as a cellular substrate of Cdk5/p25. p25 and Myc-tagged Prx-II were co-transfected in HeLa cells and expressed for either 24 or 36 h (lanes 2 and 3 respectively), followed by ³²P-orthophosphoric acid radiolabeling and isolation as described in Experimental procedures.

This step ensured that specific protein pools were enriched in different fractions. The combination of specific polypeptide labeling, 2D electrophoresis, and mass spectrometry resulted in the identification of several neuronal substrates of Cdk5. These substrates suggested diverse neurotoxic roles of Cdk5 in the brain upon deregulation (Sun *et al.* 2008, this study and K. H. Sun, unpublished data). Identification of Prx-I and Prx-II as direct substrates of Cdk5 suggested a possible role for Cdk5 in promoting oxidative stress by compromising these two anti-oxidant enzymes in brain tissues and forms the basis for the present study.

Validation of novel cdk5 substrates

Confirmation of Prx-I and Prx-II as Cdk5 substrates in the cells

Kinase substrate specificity *in vivo* is maintained by cellular localization and protein-protein interactions, thus, brain fractionation and *in vitro* kinase assays may lead to artifacts. To eliminate this possibility, we confirmed Cdk5 substrate phosphorylation in HeLa cells. Cdk5 is ubiquitously expressed but is primarily active in neurons because of the presence of its activators p35 and p39 (or their truncated forms, p25 and p29, respectively) (Lew *et al.* 1994; Tsai *et al.* 1994, 2004; Lee *et al.* 1996; Patrick *et al.* 1999; Dhavan and Tsai 2001; Cruz and Tsai 2004). However, because of the low transfection efficiency of neuronal cell lines, we took advantage of ubiquitous expression of Cdk5 in HeLa cells and transfected p25 to confirm the phosphorylation of Prx-I and Prx-II (co-expressed as myc-tagged proteins) using [γ - 32 P] orthophosphoric acid metabolic labeling. These experiments confirmed that Cdk5 activation because of p25 transfection indeed results in both Prx-I and Prx-II phosphorylation (Fig. 1b and c).

Cdk5 and oxidative stress

Prx-I and Prx-II lose their peroxidase functions upon phosphorylation by Cdk5/p25

Both Prx-I and Prx-II contain Cdk consensus phosphorylation sites and upon phosphorylation by different Cdk members, their peroxidase activities are reduced (Chang *et al.* 2002). More recently, Qu *et al.* 2007 have shown that Prx-II binds Cdk5/p35, and is phosphorylated in neurons upon MPP⁺ and/or MPTP treatment in animals, which results in reduction of its peroxidase activity (Qu *et al.* 2007). As Prx-I and Prx-II were identified as direct Cdk5 substrates in the brain and Prx-I is highly homologous to Prx-II, Prx-I may also share a similar regulatory mechanism. More specifically, as p25 is generated upon A β and glutamate stimulation, Cdk5-mediated phosphorylation of Prx-I and Prx-II should reduce their enzymatic activities resulting in ROS accumulation in the cells.

6-His-tagged Prx-I and Prx-II were generated and phosphorylated using Cdk5/p25 *in vitro*, followed by peroxidase assays at different time-points. Both Prx-I and Prx-II were highly phosphorylated by Cdk5/p25 (data not shown).

Moreover, Prx-I and Prx-II lost their ability to reduce H₂O₂ rapidly upon phosphorylation by Cdk5/p25, as reported earlier using Prx-II (Qu *et al.* 2007) (Fig. 2a).

Prx-I and Prx-II have only one serine-proline/threonine-proline phosphorylation site (T90 and T89, respectively), suggesting they should be the Cdk5 phosphorylation sites. Indeed, Qu *et al.* (2007) revealed that Prx-II is phosphorylated at T89 by Cdk5/p25. Thus, Prx-I (T90A) was generated, which should be resistant to phosphorylation (Chang *et al.* 2002; Jang *et al.* 2006). Prx-II (T89A) was created as a control. These mutant proteins were subjected to phosphorylation by Cdk5/p25 and their peroxidase activities determined. In contrast to Prx-I and Prx-II, Prx-I (T90A) and Prx-II (T89A) retained their peroxidase activities at the same level even after prolonged incubation with Cdk5/p25 (Fig. 2a) (up to 12 h, data not shown). These results confirm that Cdk5-mediated phosphorylation of Prx-I and Prx-II lead to down-regulation of its peroxidase activity. As Prx-I and Prx-II are the most abundant cytosolic anti-oxidants, deregulated Cdk5 activity because of neurotoxic insults in AD may promote ROS accumulation in the cells, resulting in oxidative stress.

Inhibition of Cdk5 prevents the loss of Prx peroxidase functions in the cells

To unravel if Cdk5 affects endogenous Prx-I and Prx-II activities in the cells, HT22 cells (immortalized mouse hippocampal cells) were used. HT22 cells are widely used as a model system to monitor intracellular ROS levels upon glutamate stimulation. These cells respond to extracellular glutamate by oxytosis, which prevents cystine uptake resulting in glutathione loss and increase in ROS levels (Tan *et al.* 1998). Glutamate activates Cdk5 via p25 formation (Fig. 2b). Our previous results have revealed that Cdk5 activation upon glutamate stimulation in HT22 cells can be inhibited by pretreatment with TAT-fusion CIP (Sun *et al.* 2008). TAT-CIP displays high specificity and no toxicity when added at approximately 200 nM concentrations (Sun *et al.* 2008).

Peroxiredoxin proteins isolated from glutamate-treated HT22 cells showed reduced peroxidase activities as expected (Fig. 2c). To confirm if the inactivation of Prx was because of activation of Cdk5, TAT-CIP was added at the time of glutamate stimulation. Roscovitine was used as a positive control although it is not monospecific for Cdk5 (Meijer *et al.* 1997). Prx proteins were isolated and peroxidase assays were conducted, which showed no change in enzymatic activities (Fig. 2c), suggesting that the endogenous Cdk5 modulates Prx peroxidase activities upon activation.

Inhibition of Cdk5 leads to reduction of ROS accumulation in HT22 cells upon glutamate stimulation

As glutamate concentration varies from 1 to 10 mM in the synaptic cleft and intraneuronal compartments (Dzubay and

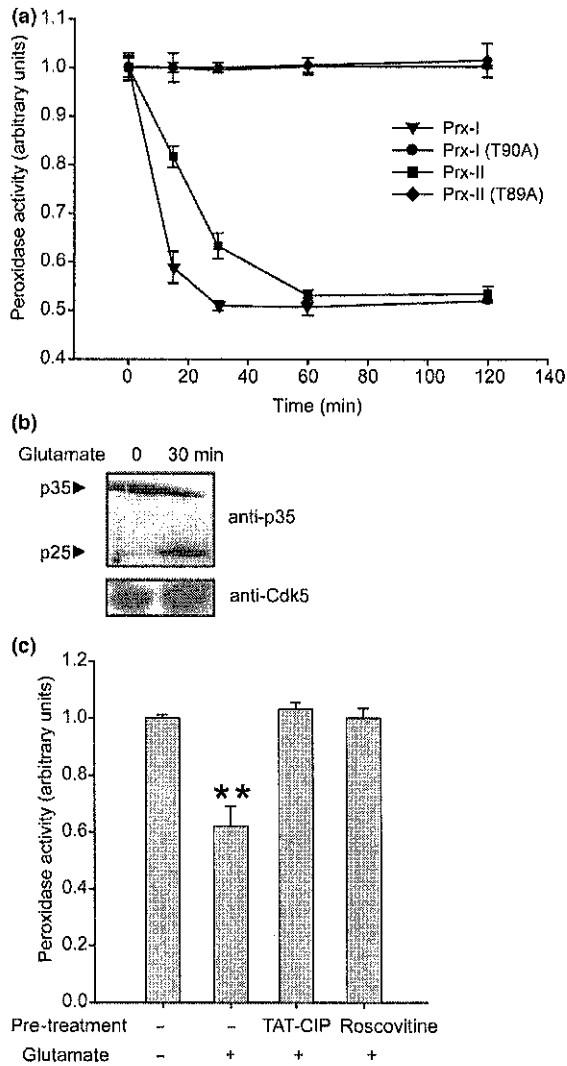


Fig. 2 Cdk5-mediated phosphorylation of Prx proteins results in the loss of peroxidase activity *in vitro*. (a) *In vitro* kinase reaction was carried out with purified Cdk5/p25 complex and Prx (-I, -II, -I-T90A, or -II-T89A) at 30°C for the indicated times. Prx peroxidase activity was measured as described in Experimental procedures. (b) HT22 cells were either untreated (lane 1) or stimulated with 5 mM glutamate for 30 min (lane 2). Whole cell lysates were separated by sodium dodecyl sulfate-polyacrylamide gel electrophoresis and transferred to polyvinylidene difluoride (PVDF) membrane. p25 and p35 were immunodetected using p35 antibody (top panel). PVDF membrane was then stripped and immunoblotted using Cdk5 antibody as a loading control (lower panel). (c) Cdk5 inhibition maintains Prx peroxidase activity inside HT22 cells. HT22 cells were pre-treated for 30 min with 200 nM TAT-Cdk5 inhibitory peptide (TAT-CIP) or 10 μ M roscovitine followed by 5 mM glutamate treatment for 4 h. Endogenous Prx was isolated by immunoprecipitation using Prx antibody (L-20), followed by peroxidase assay as described in Experimental procedures. ** $p < 0.01$.

Jahr 1999), ROS levels were monitored at 5 mM concentration. To isolate the contribution of Cdk5, TAT-CIP was used. For ROS measurement using DCFDA, TAT-mPlum-RFP which emits at 649 nm was generated as a negative control to avoid overlap at required wavelengths (Shaner *et al.* 2005; Sun *et al.* 2008). Glutamate stimulation increased ROS levels by twofold which remained at basal levels in the presence of TAT-CIP in glutamate-treated cells (Fig. 3a). TAT-RFP addition showed no effect on ROS levels. These results demonstrate Cdk5 is a key enzyme that promotes ROS accumulation upon glutamate stimulation.

Inhibition of Cdk5 leads to reduction of ROS accumulation in primary neurons upon A β and glutamate stimulation

Next, primary cortical neurons at 6 DIV, isolated from E17 CD-1 mouse embryos were subjected to glutamate stimulation. As in the case of HT22, cortical neurons do not express NMDA receptors at this stage, and glutamate toxicity is exerted by oxytosis. Similar to the results obtained in HT22 cells, ROS levels increased upon glutamate treatment and remained at basal levels if Cdk5 was inhibited during this process (Fig. 3b). TAT-RFP control showed no effect (Fig. 3b). Similar results were obtained using roscovitine (data not shown) suggesting a major role for Cdk5 in elevating ROS levels upon glutamate stimulation in primary neurons.

A β^{1-42} treatment of neuronal cells causes pathological activation of Cdk5 via p25 formation (Lee *et al.* 2000; Dhavan and Tsai 2001; Cruz and Tsai 2004; Tsai *et al.* 2004). As A β causes neurotoxicity by promoting oxidative stress, Cdk5's role in this process was investigated. In this study, A β^{25-35} was used, which is the biologically active and highly toxic core fragment of full-length A β (A β^{1-42}) (Yankner *et al.* 1990; Pike *et al.* 1995). A β^{25-35} is produced by enzymatic cleavage of naturally occurring A β in brains of AD patients (Kubo *et al.* 2002). Multiple studies have established that the toxicity and signaling events elicited by A β^{25-35} recapitulate well compared with those elicited by the physiological neurotoxic peptide A β^{1-42} . A β^{25-35} treatment resulted in more than 2.5-fold increase in ROS levels in primary cortical cells, which was Cdk5-dependent (Fig. 3c). These results suggest that Cdk5 is a key enzyme that controls oxidative stress downstream of A β and glutamate stimulation in AD, presumably via Prx-I and Prx-II phosphorylation in the cells.

Transduced TAT-Prx proteins are phosphorylated by endogenous Cdk5 inside the cells

We generated TAT-Prx-I and TAT-Prx-II to probe if excess ROS can be effectively eliminated in the cells upon glutamate stimulation. Prx-I and Prx-II were fused with TAT sequence as these proteins transduce with high efficiency and temporal control when added directly to the cells. TAT-fusion proteins build in sufficient concentrations in 30–45 min following transduction and degrade in 4–6 h (Sun *et al.* 2008). Thus, they can be added every 4 h at

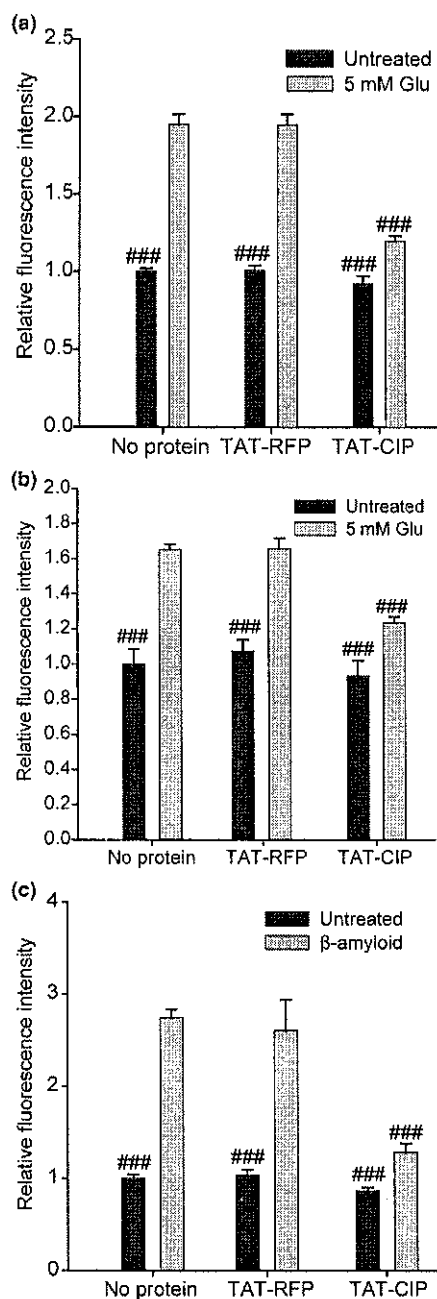


Fig. 3 Inactivation of endogenous Cdk5 results in reduction of ROS accumulation in HT22 cells and primary neurons. (a) Two hundred nanomolar of TAT-Cdk5 inhibitory peptide (TAT-CIP) or TAT-RFP was added 30 min before 5 mM glutamate (Glu) treatment in HT22 cells. After 4 h incubation, 2',7'-dichlorofluorescein diacetate (DCFDA) staining was performed as described in Experimental procedures. (b) TAT-CIP or TAT-RFP was added 30 min prior to 5 mM Glu stimulation in primary neurons, and DCFDA staining was conducted after 4 h. (c) TAT-CIP or TAT-RFP were added 30 min prior to 25 μ M β amyloid ($A\beta$)^{25–35} stimulation in primary neurons, and DCFDA staining was conducted after 4 h. ###*p* < 0.001 relative to cells treated only with Glu or $A\beta$ ^{25–35}.

approximately 200 nM concentrations to maintain constant levels in the cells (Sun *et al.* 2008).

HT22 cells were stimulated with glutamate for 4 h to induce ROS formation. To isolate the effect of Prx-I in this process, TAT-Prx-I was added 30 min prior to glutamate addition. Surprisingly, TAT-Prx-I was not efficient in reducing ROS (Fig. 4a, column 3). When TAT-Prx-I was added 3 h after glutamate, it reduced ROS levels to a small extent (column 4). However, sustained addition of TAT-Prx-I resulted in substantial decrease in ROS levels (Fig. 4a, column 6). Similar results were obtained using TAT-Prx-II (Fig. 4a). These results imply that Prx-I and Prx-II may be rendered inactive in the cells because of Cdk5-mediated phosphorylation upon glutamate stimulation.

To test this possibility, both TAT-Prx-I and TAT-Prx-II were phosphorylated *in vitro* using Cdk5/p25 and added 30 min prior to glutamate addition. Unlike TAT-Prx-I and TAT-Prx-II which showed slight decrease in ROS levels, phosphorylated TAT-Prx-I and II were ineffective in reducing ROS upon glutamate stimulation (Fig. 4b, column 4). Phosphorylation-resistant TAT-Prx-I (T90A) and TAT-Prx-II (T89A) were next generated. Transduction of either Prx-I (T90A) or Prx-II (T89A) reduced ROS to basal levels upon glutamate stimulation (Fig. 4b, column 5), suggesting that phosphorylation of T90 in Prx-I and T89 in Prx-II may cause them both to lose their peroxidase activities.

To confirm if transduced TAT-Prx proteins are rendered non-functional by elevated endogenous Cdk5 kinase activity because of neurotoxic stimulation (5 mM glutamate), TAT-Prx-transduced HT22 cells were pre-incubated with either roscovitine or TAT-CIP 30 min prior to glutamate stimulation. After 4 h, TAT-Prx proteins were isolated from cell lysates and subjected to peroxidase assays. While activation of endogenous Cdk5 by glutamate resulted in reduced peroxidase activity, inhibition of endogenous Cdk5 using either roscovitine or TAT-CIP maintained peroxidase activity of Prx proteins (Fig. 5a).

We next utilized TAT-p25 transduction, which specifically activates Cdk5 independent of any stimulus in a highly temporal fashion (Sun *et al.* 2008). Similar to the results obtained above, transduced TAT-Prx proteins lost their peroxidase activity upon TAT-p25 transduction (Fig. 5a, last column). These results verify that both Prx-I and Prx-II proteins can be phosphorylated by endogenous Cdk5 upon glutamate stimulation, which eliminate their enzymatic activities in the cells.

TAT-p25 induces oxidative stress/ROS accumulation independent of stimuli

As both Prx-I and Prx-II lose their activities upon TAT-p25 transduction, Cdk5 activity alone may be capable of increasing ROS, independent of any other input. To test this possibility, p25 was expressed in HeLa and HT22 cells using transfection and ROS level measured after 36 h. No increase

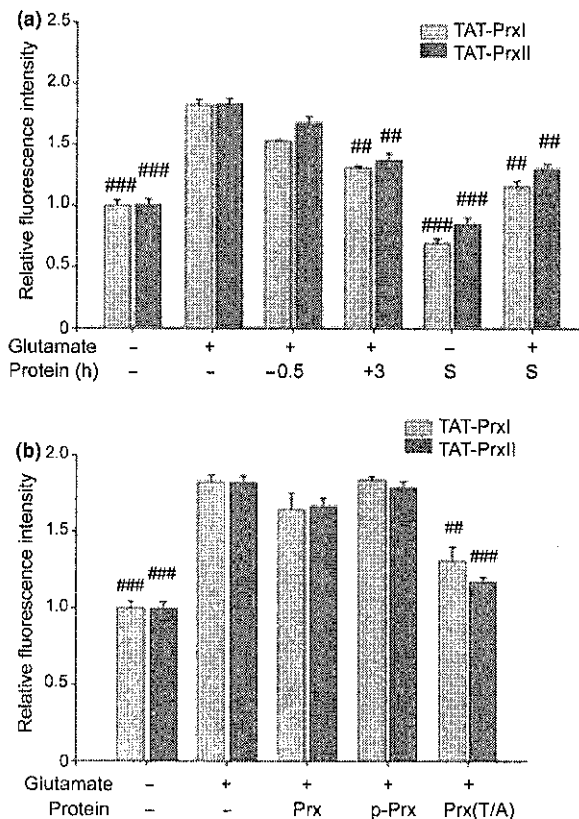


Fig. 4 Prx-I and Prx-II are inactivated by endogenous Cdk5-mediated phosphorylation, leading to ROS accumulation in the cells. (a) TAT-fusion Prx-I and Prx-II proteins were added, respectively, at indicated time in HT22 cells with or without 5 mM glutamate treatment. After 4 h, intracellular ROS was measured using 2',7'-dichlorofluorescein diacetate (DCFDA) as described in Experimental procedures. TAT-Prx was added 30 min before 5 mM glutamate stimulation, 3 h following 5 mM glutamate stimulation, or sustained addition every 1 h. (b) Intracellular ROS level was measured in HT22 cells stimulated with 5 mM glutamate in the presence of TAT-fusion proteins: unphosphorylated Prx, *in vitro* phosphorylated-Prx (p-Prx), and Prx (T/A) mutant proteins were added 30 min before glutamate stimulation. After 4 h treatment, DCFDA staining was carried out. ## $p < 0.01$, ### $p < 0.001$ compared with cells treated only with glutamate (column 2).

in ROS was observed in either cell type (data not shown), which suggested that either sole activation of Cdk5 was not sufficient to accumulate significant ROS, or cells are able to eliminate excess ROS by modulating proteins levels of antioxidant during the 36 h period.

To explore both possibilities, a tool for highly specific temporal activation of Cdk5 without causing any other perturbation to the cells was needed. Thus, TAT-p25 was used to activate Cdk5 in HT22 cells, which caused substantial increase in ROS level within 1 h (Fig. 5b). These results are important, as a recent study hypothesized that

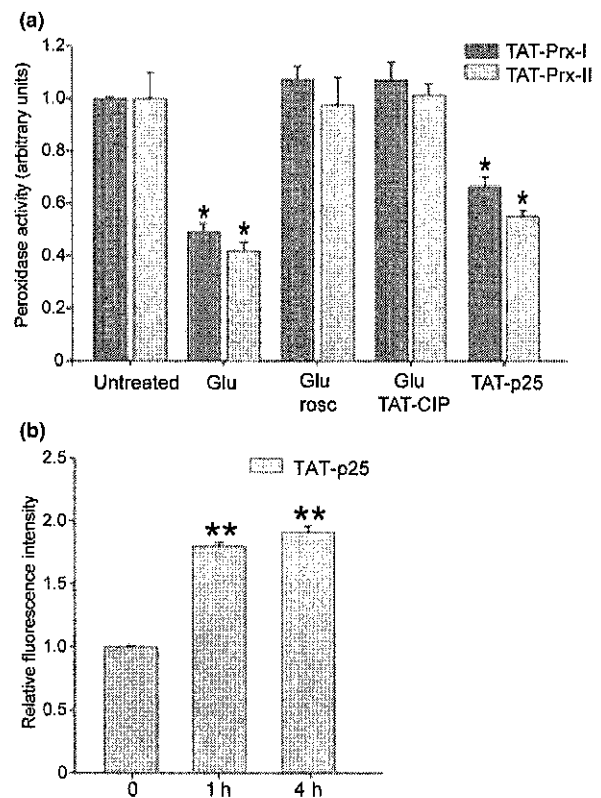


Fig. 5 Peroxidase activity of Prx-I and Prx-II proteins depends on Cdk5 activity. (a) Ten micromolar of roscovitine (rosc), 200 nM of TAT-Cdk5 inhibitory peptide (TAT-CIP) or 200 nM of TAT-p25 were added 30 min before 5 mM glutamate (Glu) stimulation and TAT-Prx addition to HT22 cells. After additional 3 h incubation, TAT-Prx was isolated from cell lysates and its peroxidase activity was determined. (b) TAT-p25 200 nM was added to the culture of HT22 cells. After 1 and 4 h, 2',7'-dichlorofluorescein diacetate staining was carried out. * $p < 0.05$, ** $p < 0.01$ compared with untreated cells.

Cdk5 induces oxidative stress downstream of mitochondrial dysfunction (Qu *et al.* 2007). In contrast, our results show that Cdk5 initiates oxidative stress and thus may be an upstream regulator of mitochondrial damage.

CDK5 and mitochondrial dysfunction

Cdk5 is upstream of mitochondrial depolarization/dysfunction upon glutamate stimulation

Cdk5 has been recently described as an effector of mitochondria, when neuronal death was induced using mitochondrial toxins (Qu *et al.* 2007). As our results indicated that TAT-p25-mediated activation of Cdk5 results in rapid ROS up-regulation, the possibility exists that it may also be independent of mitochondrial stress. Furthermore, as mitochondrial damage can be initiated by excess ROS level, we hypothesized that Cdk5 may also initiate mitochondrial dysfunction, downstream of different neurotoxic stimuli.

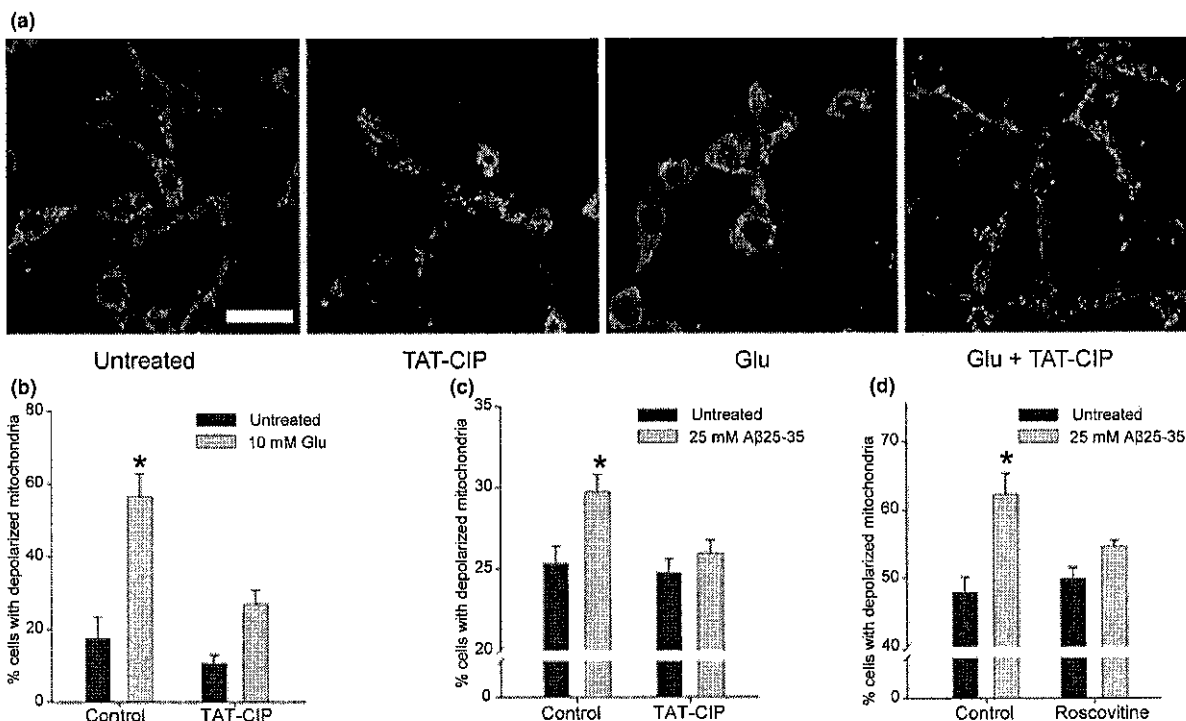


Fig. 6 Cdk5 is involved in mitochondrial depolarization following neurotoxic stimuli. (a) HT22 cells were plated for 12 h and treated with 10 mM glutamate (Glu) in the presence of 200 nM TAT-Cdk5 inhibitory peptide (TAT-CIP) or the vehicle (0.5 mM imidazole). After 10 h cells were stained with JC-1 and were analyzed using confocal microscopy: red and green fluorescence images are merged, JC-1 aggregates in polarized mitochondria appear in red, JC-1 monomer appears in green. Scale Bar: 20 μ m. (b) Quantification of cells with depolarized mitochondria scored as those without red mitochondrial staining using epifluorescence microscope as described in Experi-

mental procedures. (c) Differentiated PC12 were treated for 30 min with 200 nM TAT-CIP or 0.5 mM imidazole followed by 25 μ M β amyloid (A β) addition for 48 h and sustained addition of TAT-CIP or imidazole every 6 h. At the end of the treatment, JC-1 was added and mitochondrial polarization was measured using fluorescence-activated cell sorter. Graph shows the percentage of cells localizing in the depolarized region: decreased red/green fluorescence ratio. (d) Differentiated PC12 cells were pre-treated for 30 min with 10 μ M roscovitine or 0.1% dimethylsulfoxide and then with 25 μ M A β for 72 h, and processed as in c. * p < 0.05 compared with untreated cells.

HT22 cells were treated with glutamate in the presence or absence of TAT-CIP and mitochondrial depolarization was analyzed using JC-1 staining and confocal microscopy (Fig. 6a). While minimal mitochondrial dysfunction was observed after 6–8 h, the percentage of cells bearing depolarized mitochondria increased dramatically after 10 h (Fig. 6a and b). This phenomenon precedes glutamate-induced neuronal death (Fig. 7). Cdk5 inhibition using either roscovitine or TAT-CIP prevents mitochondrial depolarization upon glutamate stimulation, suggesting that Cdk5 is an upstream activator of mitochondrial dysfunction when subjected to neurotoxic stimulation.

Cdk5 is upstream of mitochondrial dysfunction upon A β stimulation

As glutamate-induced Cdk5 activation promoted mitochondrial depolarization, we next investigated if Cdk5 could also induce mitochondrial dysfunction upon A β ^{25–35} stimulation.

Differentiated PC12 cells were used as a model system, as sublethal concentration of A β can impair mitochondrial protein import in these cells (Sirk *et al.* 2007). When 10 μ M A β was used in differentiated PC12 cells, it caused mitochondrial membrane disruption after 72 h, but not cell death (Sirk *et al.* 2007). However, 50 μ M A β promotes significant cell death after 48 h (Choi *et al.* 2007). As A β deposition is a slow process in AD, minimum sublethal dose was used that allowed us to see a small but significant effect on mitochondrial polarization after 48–72 h, in agreement with the previous studies. PC12 cells were differentiated using NGF, treated with 25 μ M A β for 48–72 h, and mitochondrial depolarization evaluated using JC-1. Our data revealed modest mitochondrial damage (Fig. 6c and d). However, when a possible role of Cdk5 was investigated in this process, Cdk5 inhibition alleviated mitochondrial depolarization, supporting the same conclusion that Cdk5 can be upstream of mitochondrial damage in AD.

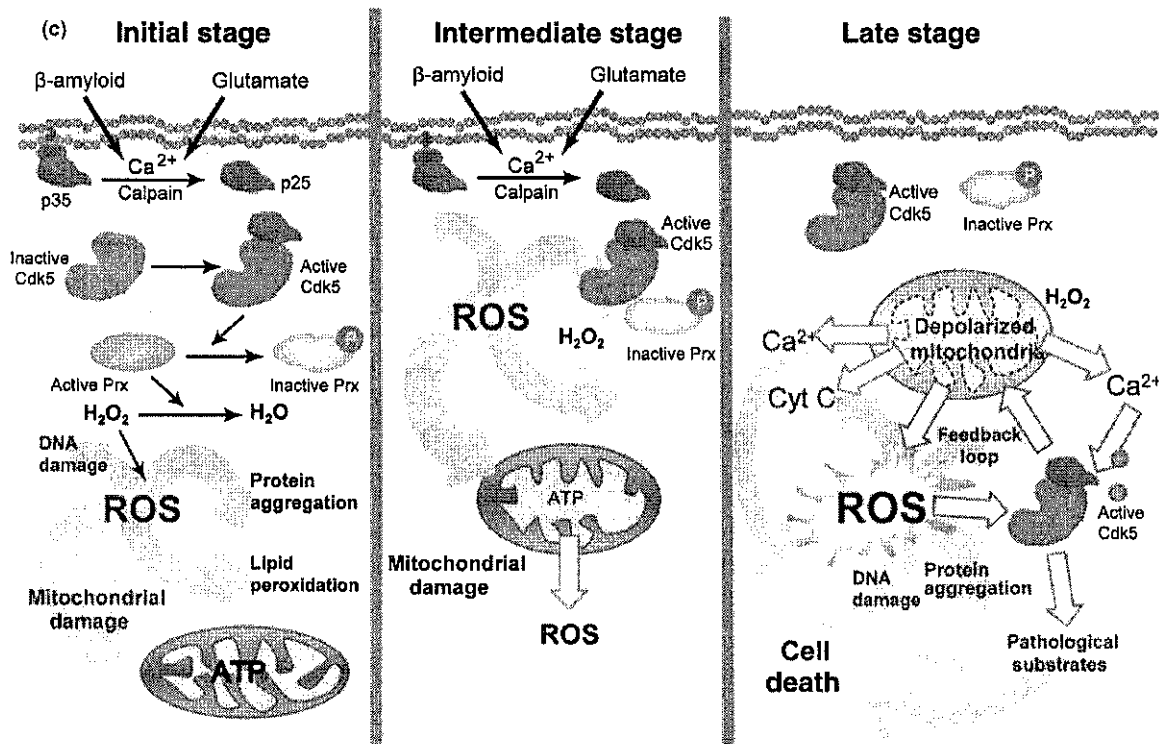
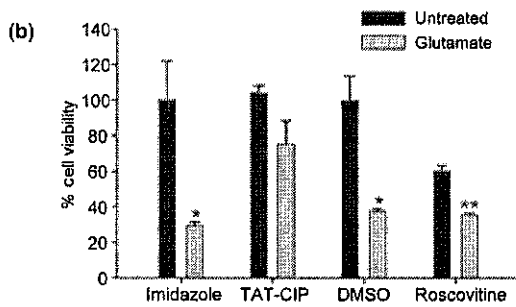
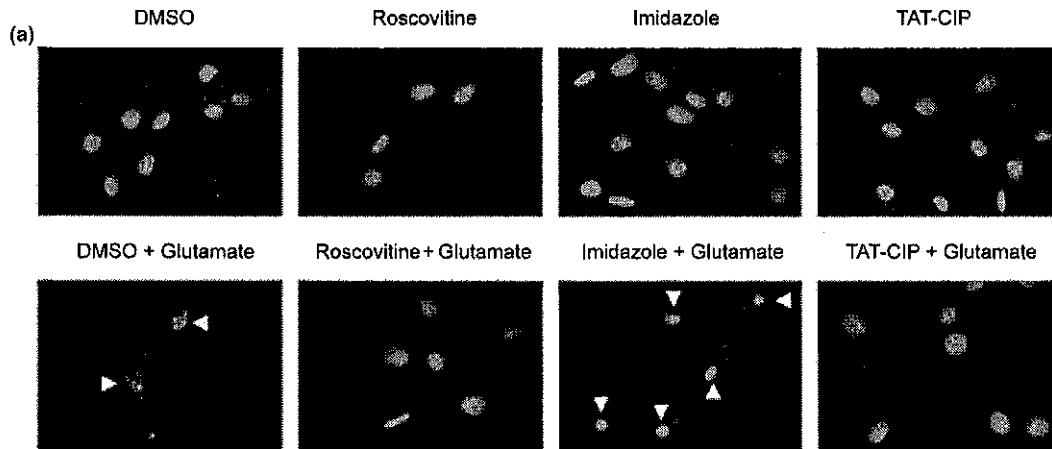


Fig. 7 Cdk5 may play a vital role in promoting neuronal death in Alzheimer's disease (AD). (a) HT22 cells were treated with 10 mM glutamate in the presence of 10 μ M roscovitine, 0.02% dimethylsulfoxide (DMSO), 200 nM of TAT-Cdk5 inhibitory peptide (CIP), or 0.1 mM imidazole for 12 h. Recombinant protein or imidazole were added every 4 h. After treatment cells were fixed, permeabilized, and nuclei were stained with propidium iodide (red). Arrow heads show apoptotic nuclei. (b) Cdk5 is involved in glutamate-induced cell death in HT22 cells. HT22 cells were pre-treated for 30 min with 200 nM TAT-CIP or its vehicle (0.5 mM imidazole) and 10 μ M roscovitine or its vehicle (0.02% DMSO), followed by 10 mM glutamate addition (gray bars). TAT-CIP or its vehicle (0.5 mM imidazole) was added every 4 h. After 18 h, cell viability was analyzed by 3-(4,5-dimethylthiazol-2-yl)-2,5-diphenyltetrazolium bromide assay, results are plotted as percentage of the untreated control. * $p < 0.05$, ** $p < 0.01$. (c) Proposed

mechanism for Cdk5's involvement in AD: (i) In the initial steps of AD, β -amyloid ($A\beta$) and excess glutamate increase the intracellular calcium activating calpain. Consequently, p35 is cleaved and Cdk5 is hyperactivated. Cdk5 phosphorylates Prx, preventing it from cleaning up the reactive oxygen species (ROS). This leads to a slow accumulation of ROS level in the cell causing oxidative stress. (ii) Mitochondria are readily damaged because of increase in ROS and Ca^{2+} levels. Mitochondrial dysfunction promotes more ROS generation and alteration of the metabolic state of the cell. (iii) In the later stage mitochondrial damage becomes irreversible, releasing more ROS and Ca^{2+} , which further activates Cdk5, which in turn contributes through a feed-back loop to generate more ROS. Cdk5 dysregulation may lead to the phosphorylation of other pathological substrates causing cell injury. Damaged mitochondria also release cytochrome c, ATP is depleted, leading to cell death.

Sole activation of Cdk5 is not enough to cause significant mitochondrial damage

As both $A\beta$ and glutamate stimulation showed a major role of Cdk5 in promoting mitochondrial damage, the next step was to test if Cdk5 deregulation alone is potent enough to cause mitochondrial damage. HT22 cells were treated with TAT-p25 for 12 h and mitochondrial dysfunction measured using JC-1. As TAT-p25 degrades in 6 h, both transient and sustained activation of Cdk5 were investigated. Although sole activation of Cdk5 can induce significant ROS formation (Fig. 5b), it was not toxic enough to cause pronounced mitochondrial damage in that time (data not shown). This result is in agreement with our previous findings showing robust Golgi fragmentation, but not significant cell death when solely Cdk5 was activated using TAT-p25 (Sun *et al.* 2008).

Cdk5 and cell death

Cdk5 inhibition rescues HT22 cells from cell death upon glutamate stimulation

As our results supported Cdk5's role in promoting cell injury upon neurotoxic insults, the next question was whether Cdk5 inhibition for extended periods could rescue cells from death. Apoptotic nuclear morphology appeared after 12 h of 10 mM glutamate addition using propidium iodide (Fig. 7a). At this time-point approximately 20% of cells showed apoptotic nuclear morphology. However, robust cell death was observed in HT22 cells after 18 h, as measured by MTT (Fig. 7b). Although both roscovitine and TAT-CIP (added every 4 h) prevented this apoptotic phenotype at 12 h (Fig. 7a), only TAT-CIP could effectively rescue the cell death as observed at 18 h (Fig. 7b). As noted earlier, roscovitine is also a potent inhibitor of Cdc2/cyclin B (IC_{50} : 650 nM) in addition to Cdk5 (IC_{50} : 200 nM), which may block cell cycle progression, leading to cell death independent of Cdk5 (Meijer *et al.* 1997). Indeed, cell

viability was reduced upon 18 h roscovitine treatment in the absence of any other neurotoxic stimulus (Fig. 7b), presumably because of sustained inhibition of Cdc2 (Fig. 7a and Sun *et al.* 2008). This finding further highlights the benefits of the temporal and specific tools used in this study.

Our results support Cdk5's role as an upstream activator of mitochondrial depolarization/dysfunction upon neurotoxic stimulation in models of AD. Mitochondrial damage leads to increase in Ca^{2+} and ROS levels, which should further activate Cdk5. Thus, we propose that Cdk5 initiates mitochondrial dysfunction upon glutamate and $A\beta$ stimulation, which further activates Cdk5 and creates a feedback loop (Fig. 7c).

Discussion

Dysregulation of Cdk5 has been suggested to play a vital role in the pathogenesis of AD (Lau and Ahljianian 2003; Cruz and Tsai 2004; Monaco 2004; Smith *et al.* 2004; Tsai *et al.* 2004). To discern the exact mechanism, we identified novel substrates of Cdk5/p25 in mouse brain extracts using a chemical genetic screen. These include Prx-I and Prx-II which suggested a possible role for Cdk5 in inducing oxidative stress in neurodegenerative diseases. Oxidative stress can further result in mitochondrial dysfunction. As both oxidative stress markers and dysfunctional mitochondria occur early in AD pathogenesis, the goal of the present study was to identify if Cdk5 is an upstream regulator or downstream effector of these phenomenon.

Oxidative stress occurs prior to the onset of significant plaque accumulation in AD (Nunomura *et al.* 2001), which is strongly supported by numerous clinical observations. Reduced mitochondrial mass and DNA content is an early pathological sign, which precedes the appearance of NFT, specifically in the neurons most vulnerable to degeneration (Nunomura *et al.* 2001). Defective energy metabolism is fundamental to AD (Bedetti 1985; Parker *et al.* 1994;

Chandrasekaran *et al.* 1996). Mitochondrial defects and decreased cytochrome oxidase activity appear to be upstream of neuronal loss (Davis *et al.* 1997). Mitochondrial dysfunction plays a pivotal role in enhancing oxidative stress. Increased ROS level triggers the opening of mitochondrial permeability transition pore and inner membrane anion channel, causing simultaneous collapse of mitochondrial $\Delta\Psi$ and a transient increase in ROS generation by the electron transport chain. Release of this ROS burst in the cytosol can activate ROS-induced ROS release in neighboring mitochondria, leading to potentially significant mitochondrial and cellular injury (Zorov *et al.* 2006).

Thus, our first objective was to investigate how Cdk5 might promote oxidative stress, downstream of A β and glutamate. As mitochondrial dysfunction plays a pivotal role in promoting ROS, the second objective was to examine if Cdk5 promotes mitochondrial damage or is activated by it. The impact Cdk5 inhibition may have on alleviating the toxicity induced by A β and glutamate to delay or even prevent cell death was the study's third objective. In pursuit of these objectives, TAT-p25 and TAT-CIP were employed to specifically activate or inhibit Cdk5 activity (Sun *et al.* 2008).

In this study, Cdk5 inhibition upon glutamate stimulation in HT22 cells and A β stimulation in primary cortical cells reduced ROS to basal levels, suggesting that upon activation, Cdk5 alone may be sufficient to induce significant oxidative damage. However, Cdk5 activation using p25 transfection in HeLa and HT22 cells failed to show any increase in oxidative stress (data not shown). Two possible explanations for this intriguing observation are sole activation of Cdk5 could not generate enough ROS or compensatory mechanisms are at play. To explore the second possibility, Cdk5 was temporally activated with TAT-p25, which led to a rapid increase in ROS levels in 1 h (Fig. 5b). We can therefore conclude that Cdk5 alone is capable of significantly increasing ROS level in the cells. This finding also emphasizes the importance of temporal tools for specific activation and inhibition of Cdk5.

Our results further show that oxidative stress induced by A β and glutamate is because of the inhibition of the peroxidase activities of Prx-I and Prx-II, which in turn are Cdk5-dependent (Fig. 4). This outcome suggested that Cdk5 could also initiate mitochondrial injury, which was investigated following A β and glutamate stimulation. In HT22 cells, glutamate caused significant mitochondrial depolarization after 10 h, which was Cdk5-dependent (Fig. 6b). Similarly, Cdk5 inhibition upon A β treatment prevented mitochondrial damage in differentiated PC12 cells. At this time-point, cell death was minimal, ruling out the possibility of the mitochondrial depolarization being a consequence rather than a cause of cell death. These data support our contention that Cdk5 is an *upstream* activator of mitochondrial dysfunction in AD. The contrast with the model proposed in Parkinson's disease by Qu *et al.* (2007) is

noteworthy. In that model, activation of Cdk5 kinase activity is *downstream* of mitochondrial dysfunction upon MPTP toxicity.

These results prompted us to examine whether sole activation of Cdk5 could cause significant mitochondrial damage. Mitochondrial dysfunction was measured in TAT-p25-treated cells at different time-points. However, no significant depolarization was observed (measured up to 12 h, data not shown). Thus, Cdk5 appears to be essential for cells to undergo mitochondrial stress, albeit only downstream of neurotoxic insults.

These results are not surprising as intraneuronal A β and glutamate can cause toxicity via several mechanisms. A β is known to interact with alcohol dehydrogenase localized in inner mitochondrial membrane which causes toxicity (Yan and Stern 2005). Similarly, previous results have shown that glutamate initially induces slow ROS formation (approximately two to three fold) in HT22 cells because of glutathione depletion. However, after 12 h of treatment, it results in huge increase in ROS level via an unknown mechanism (Tan *et al.* 1998). Thus, excess ROS formation may be an essential step that leads to mitochondrial dysfunction in HT22 cells upon glutamate stimulation. Although Cdk5 increases ROS by two-fold upon TAT-p25 transduction (Fig. 5b), this level may not be enough to cause appreciable mitochondrial damage in a short time-frame. In the context of AD pathology, Cdk5 deregulation because of neurotoxic stimuli should increase ROS level, which should result in appreciable mitochondrial damage over time.

Mitochondrial cascade hypothesis states that in sporadic late-onset AD, mitochondrial dysfunction is the primary event that causes A β deposition, synaptic degeneration, and NFT formation (Swerdlow and Khan 2004). As mitochondrial depolarization results in more ROS formation and Ca²⁺ release, both of which activate Cdk5 (Patrick *et al.* 1999; Shea *et al.* 2004), we propose that *Cdk5, via a feedback loop, is both an upstream regulator and a downstream effector of mitochondrial dysfunction*, which may ultimately promote cell death (Fig. 7c). Cdk5 dysregulation can activate additional pathogenic pathways by phosphorylating non-physiological substrates. Recent identification of GM130 as a novel substrate of Cdk5/p25, which causes Golgi fragmentation, further highlights Cdk5's role in AD (Sun *et al.* 2008). Extensive recent findings support oxidative stress, mitochondrial dysfunction, and calcium dyshomeostasis as the early contributors in AD pathology, suggesting that Cdk5 activation may be an early event in AD. Cdk5, therefore, could be a critical drug target for preventing neurodegeneration in AD.

Acknowledgements

We thank Laurent Meijer for GST-Cdk5, Steve Dowdy for pET-28b-TAT (V2.1) and pTAT-HA vectors, Roger Tsein for mPlum-RFP, and

- 5 in apoptotic and excitotoxic neuronal death. *J. Neurosci.* **25**, 8954–8966.
- Parker Jr, W. D., Mahr N. J., Filley C. M., Parks J. K., Hughes D., Young D. A. and Cullum C. M. (1994) Reduced platelet cytochrome c oxidase activity in Alzheimer's disease. *Neurology* **44**, 1086–1090.
- Patrick G. N., Zukerberg L., Nikolic M., de la Monte S., Dikkes P. and Tsai L. H. (1999) Conversion of p35 to p25 deregulates Cdk5 activity and promotes neurodegeneration. *Nature* **402**, 615–622.
- Pike C. J., Walencewicz-Wasserman A. J., Kosmoski J., Cribbs D. H., Glabe C. G. and Cotman C. W. (1995) Structure-activity analyses of beta-amyloid peptides: contributions of the beta 25–35 region to aggregation and neurotoxicity. *J. Neurochem.* **64**, 253–265.
- Praticke D., Uryu K., Leight S., Trojanowski J. Q. and Lee V. M. (2001) Increased lipid peroxidation precedes amyloid plaque formation in an animal model of Alzheimer amyloidosis. *J. Neurosci.* **21**, 4183–4187.
- Qu D., Rashidian J., Mount M. P. *et al.* (2007) Role of Cdk5-mediated phosphorylation of Prx2 in MPTP toxicity and Parkinson's disease. *Neuron* **55**, 37–52.
- Quintanilla R. A., Orellana D. I., Gonzalez-Billault C. and Maccioni R. B. (2004) Interleukin-6 induces Alzheimer-type phosphorylation of tau protein by deregulating the cdk5/p35 pathway. *Exp. Cell Res.* **295**, 245–257.
- Schinder A. F., Olson E. C., Spitzer N. C. and Montal M. (1996) Mitochondrial dysfunction is a primary event in glutamate neurotoxicity. *J. Neurosci.* **16**, 6125–6133.
- Schulz J. B., Lindenau J., Seyfried J. and Dichgans J. (2000) Glutathione, oxidative stress and neurodegeneration. *Eur. J. Biochem.* **267**, 4904–4911.
- Shah K. and Shokat K. M. (2002) A chemical genetic screen for direct v-Src substrates reveals ordered assembly of a retrograde signaling pathway. *Chem. Biol.* **9**, 35–47.
- Shah K. and Shokat K. M. (2003) A chemical genetic approach for the identification of direct substrates of protein kinases. *Methods Mol. Biol.* **233**, 253–271.
- Shah K. and Vincent F. (2005) Divergent roles of c-Src in controlling platelet-derived growth factor-dependent signaling in fibroblasts. *Mol. Biol. Cell* **16**, 5418–5432.
- Shah K., Liu Y., Deirmengian C. and Shokat K. M. (1997) Engineering unnatural nucleotide specificity for Rous sarcoma virus tyrosine kinase to uniquely label its direct substrates. *Proc. Natl Acad. Sci. USA* **94**, 3565–3570.
- Shaner N. C., Steinbach P. A. and Tsien R. Y. (2005) A guide to choosing fluorescent proteins. *Nat. Methods* **2**, 905–909.
- Shea T. B., Zheng Y. L., Ortiz D. and Pant H. C. (2004) Cyclin-dependent kinase 5 increases perikaryal neurofilament phosphorylation and inhibits neurofilament axonal transport in response to oxidative stress. *J. Neurosci. Res.* **76**, 795–800.
- Sirk D., Zhu Z., Wadia J. S., Shulyakova N., Phan N., Fong J. and Mills L. R. (2007) Chronic exposure to sub-lethal beta-amyloid (A β) inhibits the import of nuclear-encoded proteins to mitochondria in differentiated PC12 cells. *J. Neurochem.* **103**, 1989–2003.
- Smith P. D., O'Hare M. J. and Park D. S. (2004) Emerging pathogenic role for cyclin-dependent kinases in neurodegeneration. *Cell Cycle* **3**, 289–291.
- Strocchi P., Pession A. and Dozza B. (2003) Up-regulation of cDK5/p35 by oxidative stress in human neuroblastoma IMR-32 cells. *J. Cell. Biochem.* **88**, 758–765.
- Sun K. H., de Pablo Y., Vincent F., Johnson E. O., Chavers A. K. and Shah K. (2008) Novel genetic tools reveal Cdk5's major role in golgi fragmentation in Alzheimer's disease. *Mol. Biol. Cell* **19**, 3052–3069.
- Swatton J. E., Sellers L. A., Faull R. L., Holland A., Iritani S. and Bahn S. (2004) Increased MAP kinase activity in Alzheimer's and Down syndrome but not in schizophrenia human brain. *Eur. J. Neurosci.* **19**, 2711–2719.
- Swerdlow R. H. and Khan S. M. (2004) A "mitochondrial cascade hypothesis" for sporadic Alzheimer's disease. *Med. Hypotheses* **63**, 8–20.
- Tan S., Sagara Y., Liu Y., Maher P. and Schubert D. (1998) The regulation of reactive oxygen species production during programmed cell death. *J. Cell Biol.* **141**, 1423–1432.
- Tandon A., Yu H., Wang L. *et al.* (2003) Brain levels of CDK5 activator p25 are not increased in Alzheimer's or other neurodegenerative diseases with neurofibrillary tangles. *J. Neurochem.* **86**, 572–581.
- Taniguchi S., Fujita Y., Hayashi S., Kakita A., Takahashi H., Murayama S., Saïdo T. C., Hisanaga S., Iwatsubo T. and Hasegawa M. (2001) Calpain-mediated degradation of p35 to p25 in postmortem human and rat brains. *FEBS Lett.* **489**, 46–50.
- Thurman R. G., Ley H. G. and Scholz R. (1972) Hepatic microsomal ethanol oxidation. Hydrogen peroxide formation and the role of catalase. *Eur. J. Biochem.* **25**, 420–430.
- Tsai L. H., Delalle I., Caviness V. S., Jr, Chae T. and Harlow E. (1994) p35 is a neural-specific regulatory subunit of cyclin-dependent kinase 5. *Nature* **371**, 419–423.
- Tsai L. H., Lee M. S. and Cruz J. (2004) Cdk5, a therapeutic target for Alzheimer's disease? *Biochim. Biophys. Acta* **1697**, 137–142.
- Tseng H. C., Zhou Y., Shen Y. and Tsai L. H. (2002) A survey of Cdk5 activator p35 and p25 levels in Alzheimer's disease brains. *FEBS Lett.* **523**, 58–62.
- Veal E. A., Day A. M. and Morgan B. A. (2007) Hydrogen peroxide sensing and signaling. *Mol. Cell* **26**, 1–14.
- Wei W., Wang X. and Kusiak J. W. (2002) Signaling events in amyloid beta-peptide-induced neuronal death and insulin-like growth factor 1 protection. *J. Biol. Chem.* **277**, 17649–17656.
- Yan S. D. and Stern D. M. (2005) Mitochondrial dysfunction and Alzheimer's disease: role of amyloid-beta peptide alcohol dehydrogenase (ABAD). *Int. J. Exp. Pathol.* **86**, 161–171.
- Yankner B. A., Duffy L. K. and Kirschner D. A. (1990) Neurotrophic and neurotoxic effects of amyloid beta protein: reversal by tachykinin neuropeptides. *Science* **250**, 279–282.
- Yoo B. C. and Lubec G. (2001) p25 Protein in neurodegeneration. *Nature* **411**, 763–764 (Discussion 764–765).
- Zheng Y. L., Li B. S., Amin N. D., Albers W. and Pant H. C. (2002) A peptide derived from cyclin-dependent kinase activator (p35) specifically inhibits Cdk5 activity and phosphorylation of tau protein in transfected cells. *Eur. J. Biochem.* **269**, 4427–4434.
- Zheng Y. L., Kesavapany S., Gravel M., Hamilton R. S., Schubert M., Amin N., Albers W., Grant P. and Pant H. C. (2005) A Cdk5 inhibitory peptide reduces tau hyperphosphorylation and apoptosis in neurons. *EMBO J.* **24**, 209–220.
- Zhu X., Su B., Wang X., Smith M. A. and Perry G. (2007) Causes of oxidative stress in Alzheimer disease. *Cell. Mol. Life Sci.* **64**, 2202–2210.
- Zorov D. B., Juhaszova M. and Sollott S. J. (2006) Mitochondrial ROS-induced ROS release: an update and review. *Biochim. Biophys. Acta* **1757**, 509–517.

To PULSe Award Committee

Reference: Sun KH, de Pablo Y, Vincent F, and Shah K. (2008) Deregulated Cdk5 Promotes Oxidative Stress and Mitochondrial Dysfunction. *Journal of Neurochemistry* 107, 265-278.

Significance of this study: Alzheimer's Disease (AD) is a fatal neurodegenerative disorder. However, the exact mechanism of extensive neuronal cell death remains to be fully elucidated. Oxidative stress is believed to be one of the earliest contributors of AD pathology. In this study, we conducted a chemical genetic screen and reported the crucial role of cyclin-dependent kinase 5 (Cdk5) in promoting oxidative stress upon deregulation via compromising the cellular antioxidant defense system in the AD model. Furthermore, with the aid of Cdk5 modulators developed previously in our laboratory (Sun KH *et al.* 2008 *Molecular Biology of the Cell* 19, 3052-69), our study revealed that Cdk5 as an upstream regulator of mitochondrial dysfunction, which lead us to propose a model showing a feedback loop between Cdk5 and oxidative stress, which may occur in the late stage of AD causing neuronal cell death.

Kai-Hui's authorship in this study: Kai-Hui Sun is the first author in this paper. She contributed more than 90% of work in this study.

Identification of two pathological substrates of Cdk5: Our chemical genetic screen identified two antioxidant enzymes, peroxiredoxin-I and -II (Prx-I and Prx-II), as Cdk5 direct substrates, which suggests a potential linkage between Cdk5 and oxidative stress. These substrates were identified by a former postdoctoral associate Fabien Vincent. Kai-Hui cloned both Prx-I and Prx-II, and subjected them to an *in vitro* Cdk5 kinase assay, respectively, and confirmed that Prx-I and Prx-II are indeed Cdk5's substrates. She subsequently conducted a series of peroxidase assays and showed that Cdk5-mediated phosphorylation of Prx-I/Prx-II inactivates their abilities to clean up cellular reactive oxygen species (ROS) (Fig. 2a). These results suggest that Cdk5 may participate in production of ROS in neurons upon deregulation.

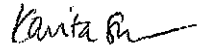
Discovery of Cdk5's role in promoting oxidative stress: To verify the role of Cdk5 in promoting oxidative stress in neurons, Kai-Hui tracked the cellular ROS levels following treatment of neurotoxicity with and without inhibition of Cdk5. Her results demonstrated that inhibition of Cdk5 reduces ROS accumulation (Fig. 2c and Fig. 3), indicating a crucial of Cdk5 in promoting oxidative stress.

Later, to further reveal the mechanism of Cdk5-mediated oxidative stress, Kai-Hui generated TAT-fused wild-type and mutant Prx proteins, which enable efficient transduction and high temporal control when added to the neuronal cells. Her results indicated that Cdk5-mediated ROS accumulation is due to inactivation of Prx proteins (Fig. 4a-4c). Finally, Kai-Hui along with our previous post-doctoral fellow, Dr. Yolanda de Pablo, also performed an assay of nuclear condensation to further confirm that Cdk5 plays a vital role in neuronal cell death (Fig 5). Kai-Hui also provided inputs for the proposed model (Fig. 5c).

Kai-Hui's additional contributions to publication: Kai also played a major role in writing this manuscript. Since the publication of this study, we have received several requests from other research groups for TAT-fusion Prx proteins which were developed by Kai-Hui. Overall, Kai-

Hui was the major contributor in this study, which uncovered the mechanism by which Cdk5 promotes oxidative stress and mitochondrial dysfunction upon deregulation, which may ultimately lead to neurodegeneration in AD.

Sincerely,

A handwritten signature in black ink, appearing to read "Kavita Shah", with a stylized flourish at the end.

Kavita Shah, Ph.D.